Preprints of the 19th World Congress
The International Federation of Automatic Control
Cape Town, South Africa. August 24-29, 2014

Current Scheduling for Parallel Buck Regulated Battery Modules

Xin Zhao * **Raymond A. de Callafon** * **Lou Shrinkle** **

* *Department of Mechanical and Aerospace Engineering*
University of California, San Diego
9500 Gilman Drive, La Jolla, CA 92093-0411, USA
** *1856 Wilstone Ave, Encinitas, CA 92024, USA*

Abstract: In an electrical energy storage and delivery system, a parallel connection of battery modules can be used to increase the storage capability and power delivery demands. Parallel connection of batteries requires a robust battery management system as batteries may have different operating parameters such as state-of-charge (SoC), open-circuit voltage (OCV), internal resistance or battery chemistry. This paper focuses on current scheduling for a parallel connection of battery modules by utilizing buck regulators in the battery management system (BMS) of each module to improve the system performance via simultaneous, sequential and hybrid discharge scheduling algorithms. The results indicate the feasibility of the scheduling algorithms and motivate the use of parallel connected battery modules despite changes in battery operating parameters.

Keywords: Exchangeable parallel battery module; Current scheduling; Electric Vehicle; Quadratic programming; Pulse-width modulation.

1. INTRODUCTION

Electrical energy storage and delivery systems (EESDS) are important in industrial applications that include power grids, second life battery systems, and electric vehicles (Bragard et al., 2010; Smith and Wang, 2006; Lacey et al., 2013) with intermittent power delivery demands. The development of high-performance battery cells (Armand and Taracson, 2008) and advanced battery management technologies (Chaturvedi et al., 2010) make batteries critical components in enhancing the performance of EESDS.

As the bus voltage of an EESDS is typically constrained, a parallel connection of battery modules is a solution to increase the energy storage capability and the delivered power. For instance, in Battery Electric Vehicles (BEV), the power-train is driven purely by electric power, thus a parallel battery architecture is especially needed to fulfil the capacity and power requirements to ensure an acceptable range and the performance of vehicles (Khaligh and Li, 2010). Similar parallel connection of batteries with different operating parameters can be found in second life applications to provide ancillary grid services.

Currently, parallel battery modules are mostly formed as one compact pack, which is applicable for small-scale applications such as portable devices. However, a compact battery pack employed in the large-scale implementation results in a maintenance problem, that is, replacing a portion of the battery pack is either not feasible or fairly complicated in practice. While the technology of fast charging battery cells is evolving quickly (Kang and Ceder, 2009), there still exists some significant challenges for fast charging large-scale battery packs (Botsford and Szczepanek, 2009).

A battery architecture with exchangeable modular and parallel connected batteries is a promising solution for increasing storage capacity. Instead of forming all the battery cells into one pack, the pack is sectioned into several independent modules that are designed to be exchangeable. Multiple such modules are connected in parallel onto the bus, as shown in Fig. 1. With the implementation of such architecture, the robustness of the battery system is enhanced significantly: when a cell or a module failure occurs, a portion of the battery pack is exchangeable, which also reduces the cost of maintenance. Furthermore, the possibility of rapidly exchanging battery modules shortens the wait time to obtain a fully-charged battery system, which is a critical requirement for the feasibility of long-distance travel with a BEV.

The exchangeable modular battery architecture poses several challenges for the battery management system. By replacing one or multiple battery modules, each module may have different SoCs, i.e., the ratio of the instantaneous battery capacity over its nominal capacity. Furthermore, the cells of each module may be built with different materials, thus have different electrochemical characteristics such as charging and discharging profiles (Nishi, 2001). These ingredients lead to scheduling issues when charging or discharging battery modules. In addition, the internal impedance in each battery module causes power loss, hence the control of these modules can also be formulated as an optimization problem to minimize energy loss that can be solved by Quadratic Programming (QP) (Mehrotra, 1992; Ye, 2002), Semidefinite Programming (SDP) (Bai

⋆ E-mail contact: xiz028@ucsd.edu; callafon@ucsd.edu

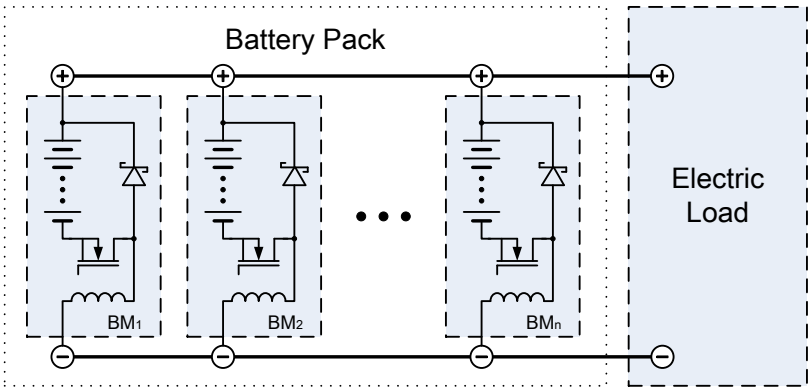

Fig. 1. System diagram of parallel buck regulated battery modules. In each module, the battery is represented by a series connection of battery cells to create the desired OCV, while a BMS with metal-oxide-semiconductor field-effect transistor (MOSFET) microcontroller controlled switch with a fly-by diode and inductor are used for regulation of the battery voltage on the parallel bus.

et al., 2008), depending on the constraints taken into consideration.

There exist several solutions to similar scheduling problems in the literature. For instance, a thorough solution of a stand-alone energy storage system with parallel battery architecture is proposed via on/off switching control in Kaiser's (Kaiser, 2007). The approach in this paper, however, provides a new level of control by actively managing the individual power flow of each module via Pulse-Width Modulation (PWM) control. In the paper, the battery system is first modeled for current scheduling. Then the scheduling algorithms under constrained DC bus voltage are introduced, including simultaneous, sequential, and hybrid algorithms for discharge scheduling. Finally, the scheduling algorithms are simulated in a dynamic power demand simulation using a driving profile of a BEV.

2. PARALLEL BUCK REGULATED BATTERY MODULES

2.1 Model Formulation

In this paper, the current scheduling of parallel battery modules is executed by buck regulators, which is composed by a pulse-width modulated MOSFET, a fly-by diode, and an inductor, as indicated in Fig. 1. In each battery module, the battery cells are connected in series and then buck regulated. Several such battery modules are connected in parallel by DC bus, which ultimately form a battery pack and is connected to the electric load.

Notice that the number of modules n is arbitrary, which means that the battery pack can be fully or partially loaded with battery modules. This feature further enhances the flexibility of the application of such battery system.

For the derivation of the current scheduling algorithm, the system of parallel buck regulated battery modules is approximated as a parallel connection of adjustable power supplies, as indicated in Fig. 2. Specifically, each battery module with a serial of multiple cells is modeled as two components in serial: an ideal battery with an open-circuit voltage $V_{OC,i}$ and an internal resistance R_i (Gao et al., 2002), where $i = 1, 2, \ldots, n$, which essentially influences the current scheduling. The open-circuit voltage is buck regulated to a lower voltage

$$V_i = D_i \cdot V_{OC,i}$$

where D_i is the PWM duty cycle of MOSFET, and $D_i \in [0, 1]$.

2.2 Formulation of Constraints

With the formulated model, the system constraints can be derived. Applying Kirchhoff's laws yields

$$V_i - R_i \cdot I_i + R_{i+1} \cdot I_{i+1} - V_{i+1} = 0 \tag{1}$$

where $i = 1, 2, \ldots, n-1$, and

$$V_n - R_n \cdot I_n - V_{bus} = 0 \tag{2}$$

$$\sum_{i=1}^{n} I_i = I_{bus} \tag{3}$$

(1) - (3) formulate the fundamental equalities for the system. In addition, there exist inequality constraints in the system. Since $D_i \in [0, 1]$, the voltage constraint for each battery module is:

$$0 \leqslant V_i \leqslant V_{OC,i} \tag{4}$$

Furthermore, there also exists the current constraint for each module due to the limitations of the battery cells:

$$0 \leqslant I_i \leqslant I_i^{\max} \tag{5}$$

Notice that the inequality constraints are intended to be independent for each module, since the current scheduling

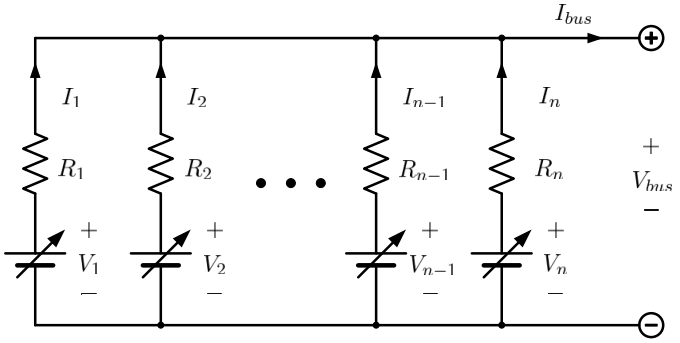

Fig. 2. Model for current scheduling

is aimed to be applicable for implementation on battery modules with different operating parameters such as SoC, internal resistance and moreover, with different electro-chemical features.

Accordingly, the current scheduling is generally to determine the feasible solution that is subject to (1) - (3) with the constraints (4) and (5). The constraints are subject to change depending on the actual system design.

3. CURRENT SCHEDULING ALGORITHMS UNDER CONSTRAINED DC BUS VOLTAGE

In some applications, the electric load imposes constraints on the DC bus voltage:

$$V_{bus}^{\min} \leqslant V_{bus} \leqslant V_{bus}^{\max} \tag{6}$$

In practice, the SoC of each module is evaluated and utilized as a crucial reference (Lin et al., 2013; Moura et al., 2012). Therefore, the SoC of each module is taken into account while determining the scheduling strategy. Furthermore, the real-time SoC and internal resistance can be estimated and applied for control purpose (Sitterly et al., 2011), which enables the implementation of on-line scheduling.

3.1 Simultaneous Discharge (SimD) Scheduling

The SimD scheduling is defined by a current of each module scheduled according to

$$I_i = \alpha_i \cdot I_{bus} \tag{7}$$

where the current scheduling ratio α_i is given by

$$\alpha_i = \frac{\mathrm{SoC}_i}{\sum_{i=1}^{n} \mathrm{SoC}_i}. \tag{8}$$

It means that the modules with higher SoC are scheduled to deliver more current, while the ones with lower SoC can operate at a relatively low rate. Intuitively, all the modules ultimately deplete completely at the same time. Clearly the SimD scheduling causes a simultaneous and constant current delivery for each module when the bus current is required to be constant.

By (1) and (2), once the current of each module I_i is determined, the buck regulated voltage of each module V_i is essentially determined by V_{bus}:

$$V_i = V_{bus} + R_i \cdot I_i \tag{9}$$

where $i \in \{1, 2, \ldots, n\}$ and V_{bus} is constrained by (6).

Toggling the MOSFETs introduces undesirable parasitic power loss and decreases the module efficiency, hence at least one MOSFET should be set to operate in the full duty cycle, that is, to find a feasible solution under the equality constraint $V_i = V_{OC,i}$, which is transformed from one of the inequality constraints (4).

The SimD scheduling is illustrated by a constant current demand simulation as shown in Fig. 3. The desired bus current is 100A. Initially, the SoC of the modules are 100%, 55%, 90%, and 45%, respectively in this illustration. Although such different initial SoCs is not quite realistic in most operating conditions, it is easier to distinguish for demonstration purposes. Moreover, such conditions may exist, for instance, in second life applications for used EV battery modules.

The SoC threshold for discharge is set to 10%, hence the current of each module is determined by (7) with available SoC. Furthermore, the OCV and internal resistance of each module is assumed to vary linearly with the SoC in the simulation. Specifically, the OCV decreases and the internal resistance increases as the battery discharges. As expected, all the modules are completely discharged at the same time, and the proportion of SoC between each module is the same along the battery discharge.

3.2 Sequential Discharge (SeqD) Scheduling

Battery modules do not necessarily have to be discharged in a simultaneous pattern and an alternative SeqD scheduling can be used to discharge battery modules sequentially. Such algorithm aims to deplete the battery modules one by one. Specifically, SeqD scheduling starts depleting the module with the lowest SoC. If the output current of the module with the lowest SoC is lower than the required bus

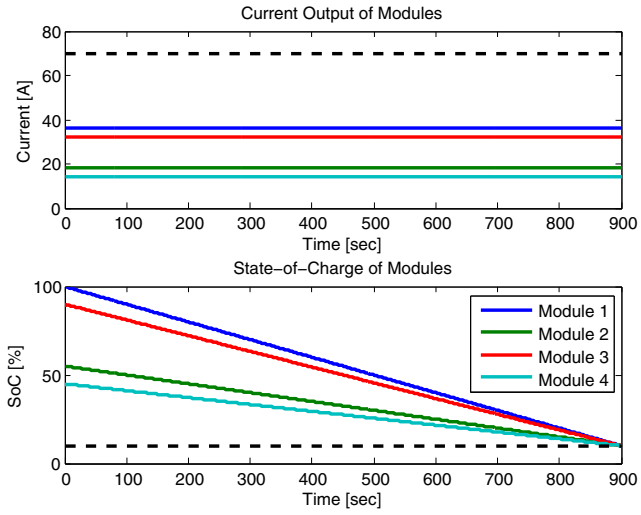

Fig. 3. SimD scheduling for constant current demand with current in each module in top figure and SoC in bottom figure. Dashed lines indicate constraints.

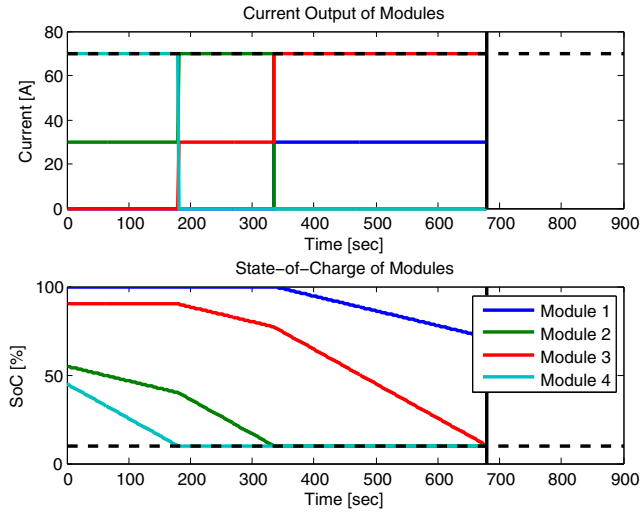

Fig. 4. SeqD scheduling for constant current demand with current in each module in top figure and SoC in bottom figure. Dashed lines indicate constraints.

current, then the modules are iteratively implemented one after another till the current demand is fulfilled.

The SeqD scheduling is also demonstrated by a constant current demand simulation as shown in Fig. 4. The conditions of each module are the same as in the simulation for SimD. The desired bus current is still 100A. Since the maximum output current of the modules is set to 70A, one module is not able to fulfil the current demand. Starting with the discharging of Module 4, the modules are discharged one by one. For instance, at 350 seconds, Module 4 and Module 2 are discharged to the minimum level of 10% SoC while Module 3 has relatively high SoC and Module 1 is still fully-charged. Therefore, by replacing two out of four modules, a fully charged battery pack is obtained, demonstrating the usefulness of the SeqD scheduling.

However, the number of functioning modules decreases as more modules are completely discharged, which results in the infeasibility of fulfilling high current demand. In the constant current demand simulation, three modules stop functioning after approximately 680 seconds. Although the remaining module operates at the maximum output current, the bus current demand cannot be achieved. Therefore the operation of battery system is terminated. This is considered to be the drawback of such scheduling algorithm, since it sacrifices the power capability, especially when a large portion of modules are out of service. But the SeqD algorithm is still useful for some applications with relatively low power demand and the possibility of frequent exchange of battery modules, such as the daily urban transportation by BEV, since a fully-charged battery pack can be obtained by exchanging a portion of the modules rather than all of them.

3.3 Hybrid Discharge (HybD) Scheduling

Since there exists power loss due to internal resistance:

$$P_{\text{loss}} = \sum_i (I_i^2 R_i) \tag{10}$$

the current scheduling can take account of such power loss to motivate a scheduling that aims to minimize the power loss in (10).

Introducing slack variables u_i, l_i, w_1, w_2, (4), (5), and (6) can be rewritten as:

$$\begin{aligned} V_i + u_i &= V_{OC,i}, \quad V_i \geqslant 0, \quad u_i \geqslant 0 \\ I_i + l_i &= I_i^{\max}, \quad I_i \geqslant 0, \quad l_i \geqslant 0 \\ V_{bus} + w_1 &= V_{bus}^{\max}, \quad w_1 \geqslant 0 \\ V_{bus} - w_2 &= V_{bus}^{\min}, \quad w_2 \geqslant 0 \end{aligned}$$

where $i \in \{1, 2, \ldots, n\}$. The unknowns can be grouped into $x \in \mathbb{R}^{4n+3}$: $x = \begin{bmatrix} x_1^T & x_2^T & x_3^T & x_4^T & x_5^T \end{bmatrix}^T$, where

$$\begin{aligned} x_1 &= [V_1 \ V_2 \ \cdots \ V_n]^T, \quad x_2 = [I_1 \ I_2 \ \cdots \ I_n]^T \\ x_3 &= [u_1 \ u_2 \ \cdots \ u_n]^T, \quad x_4 = [l_1 \ l_2 \ \cdots \ l_n]^T \\ x_5 &= [V_{bus} \ w_1 \ w_2]^T \end{aligned}$$

Thus, all the equality and inequality constraints for the system can be formulated into:

$$Ax = b, \quad x \geqslant 0$$

where $A \in \mathbb{R}^{(3n+3)\times(4n+3)}$:

$$A = \begin{bmatrix} A_1 & A_2 & 0 & 0 & A_3 \\ I & 0 & I & 0 & 0 \\ 0 & I & 0 & I & 0 \\ 0 & 0 & 0 & 0 & A_4 \end{bmatrix}$$

and

$$A_1 = \begin{bmatrix} 1 & -1 & 0 & \cdots & 0 \\ 0 & 1 & -1 & \cdots & 0 \\ \vdots & \vdots & \ddots & \ddots & \vdots \\ 0 & 0 & \cdots & 1 & -1 \\ 0 & 0 & \cdots & 0 & 1 \\ 0 & 0 & \cdots & 0 & 0 \end{bmatrix}$$

$$A_2 = \begin{bmatrix} -R_1 & R_2 & 0 & \cdots & 0 \\ 0 & -R_2 & R_3 & \cdots & 0 \\ \vdots & \vdots & \ddots & \ddots & \vdots \\ 0 & 0 & \cdots & -R_{n-1} & R_n \\ 0 & 0 & \cdots & 0 & -R_n \\ 1 & 1 & \cdots & 1 & 1 \end{bmatrix}$$

$$A_3 = \begin{bmatrix} 0 & \cdots & 0 & -1 & 0 \\ 0 & \cdots & \cdots & \cdots & 0 \\ 0 & \cdots & \cdots & \cdots & 0 \end{bmatrix}^T$$

$$A_4 = \begin{bmatrix} 1 & 1 & 0 \\ 1 & 0 & -1 \end{bmatrix}$$

The internal resistance of each module $R_i \in \mathbb{R}_+$, therefore it can be verified that A has full rank. Furthermore, since $R_i \in \mathbb{R}_+$, Q is positive semidefinite, the current scheduling can be formulated as a Quadratic Programming (QP) problem:

$$\begin{aligned} \text{minimize} \quad & q(x) = \frac{1}{2} P_{\text{loss}} = \frac{1}{2} x^T Q x \\ \text{subject to} \quad & Ax = b, \\ & x \geqslant 0. \end{aligned}$$

where $Q \in \mathbb{S}^{4n+3}$:

$$Q = \begin{bmatrix} 0 & & & & \\ & R & & & \\ & & 0 & & \\ & & & 0 & \\ & & & & 0 \end{bmatrix}$$

and

$$R = \begin{bmatrix} R_1 & 0 & \cdots & 0 \\ 0 & R_2 & \cdots & 0 \\ \vdots & \vdots & \ddots & \vdots \\ 0 & 0 & \cdots & R_n \end{bmatrix}$$

Due to the convexity of the QP, the minimization of (10) under constraints is solvable by algorithms such as Path-Following algorithm, Potential-Reduction algorithm (Ye, 2002), or Reflective Newton method (Coleman and Li, 1996).

The constant current demand simulation is executed with the scheduling introduced above and results are shown in Fig. 5. It is observed that the battery modules deplete in a sequential pattern and the range increases by 29% comparing with the terminate time of SeqD scheduling. Such scheduling algorithm balances the range and the depleting mode, hence it is called Hybrid Discharge (HybD) scheduling. On the basis of all the constant current demand simulations, the total energy losses due to internal

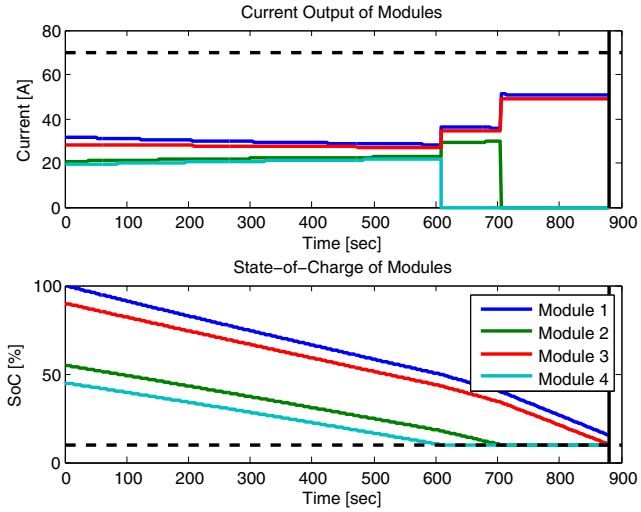

Fig. 5. HybD scheduling for constant current demand with current in each module in top figure and SoC in bottom figure. Dashed lines indicate constraints.

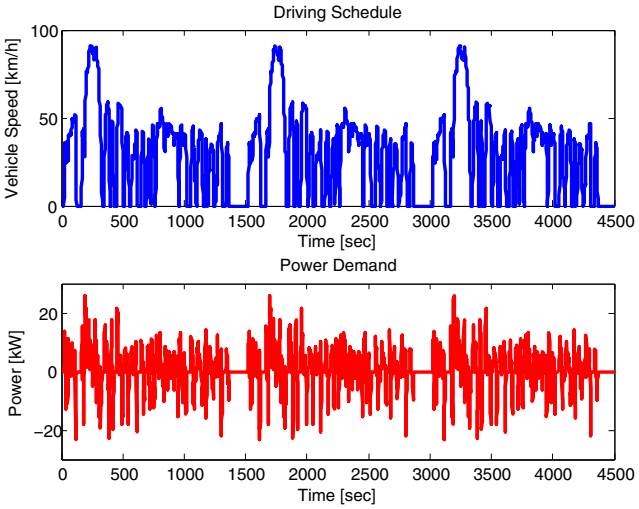

Fig. 6. Driving profile and power demand (UDDS)

resistance for the first 600 seconds are listed in Table 1. SeqD scheduling results in the largest energy loss since at least one module is operating at the maximum output current at a time. The energy loss is decreased from SimD scheduling to HybD scheduling. Considering that the internal resistance given in the simulation is in the order of several mΩ, the decrease of approximately 7% is noteworthy.

Table 1. Comparison of Energy Losses

Current Scheduling Algorithm	Energy Loss (kJ)
SimD scheduling	177.67
SeqD scheduling	417.67
HybD scheduling	165.36

4. DYNAMIC POWER DEMAND SIMULATION FOR CURRENT SCHEDULING ALGORITHMS

In the previous section, a constant current demand test is utilized for demonstration of the different current scheduling algorithms. Even for dynamic current demand cases, the three proposed algorithms are solvable. For that purpose, we also consider applying these algorithms to dynamic power demand cases, which are required in applications with intermittent power delivery demands such as BEVs.

The EPA Urban Dynamometer Driving Schedule (UDDS) is applied to demonstrate the current scheduling for a variable power demand as indicated in Fig 6. The driving schedule includes the vehicle speed information along a virtual urban route, the derivative of which can be considered as the sum of vehicle accelerations driven by powertrain and slope. Given the acceleration, the power demanded by the vehicle can be calculated by the propulsion equation of vehicles:

$$P_{des} = (M \cdot a + C_r \cdot M \cdot g + C_a \cdot \frac{A}{21.15} \cdot v^2) \cdot v \qquad (11)$$

where M is the mass of the vehicle, a is the required acceleration, C_r is the coefficient of rolling, g is the gravity constant, C_a is the coefficient of air resistance, A is the frontal area of the vehicle, v is the required velocity of the vehicle.

The desired power demand is for the entire battery system, since V_{bus} and I_{bus} are uncertain, we have:

$$V_{bus} \cdot I_{bus} = P_{bus} = P_{des} \qquad (12)$$

Due to the product of the unknown bus voltage and current, current scheduling is more challenging, but can be solved for the SimD and SeqD scheduling trivially.

For SimD scheduling, by (2) and (7), assuming $V_n = V_{OC,n}$ yields:

$$V_{OC,n} - \alpha_n \cdot R_n \cdot I_{bus} = V_{bus} \qquad (13)$$

Combining (12) and (13), the bus current can be obtained by solving a quadratic equation:

$$I_{bus} = \frac{V_{OC,n} \pm \sqrt{V_{OC,n}^2 - 4 \cdot P_{des} \cdot \alpha_n \cdot R_n}}{2 \cdot \alpha_n \cdot R_n} \qquad (14)$$

Thus, the bus voltage V_{bus} can also be determined. If there exists no feasible solution due to the inequality constraints (4) - (6), then it is assumed that other modules operate at the full duty cycle and resolve (14) iteratively.

For SeqD scheduling, when one battery module with the lowest SoC cannot fulfil the power demand, more modules can be iteratively implemented. For the implemented modules, the current of each module can also be determined by (14).

The simulation results for the SimD and SeqD scheduling algorithms are summerized in Fig 7 and Fig 8. The results indicate the feasibility of the scheduling algorithms, where the SimD scheduling depletes all the modules at the same time, while the SeqD scheduling discharges the modules in a sequential manner.

5. CONCLUSION

Several current scheduling algorithms for a system comprised by parallel connected battery modules are discussed in this paper. By formulating the constraints of such system under constrained DC bus voltage, the simultaneous

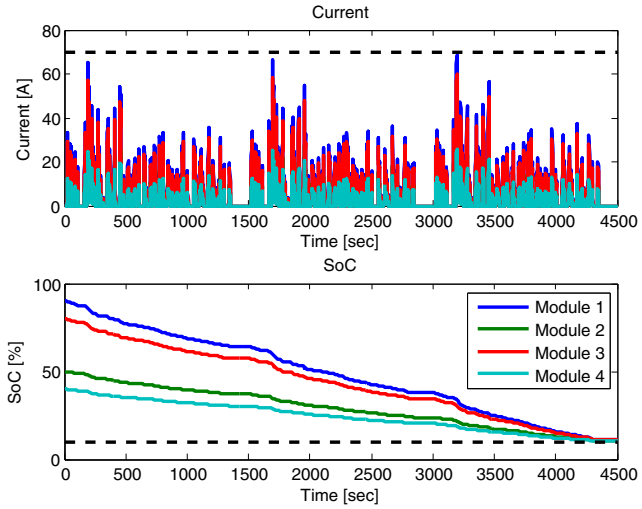

Fig. 7. SimD Scheduling for Dynamic Power Demand

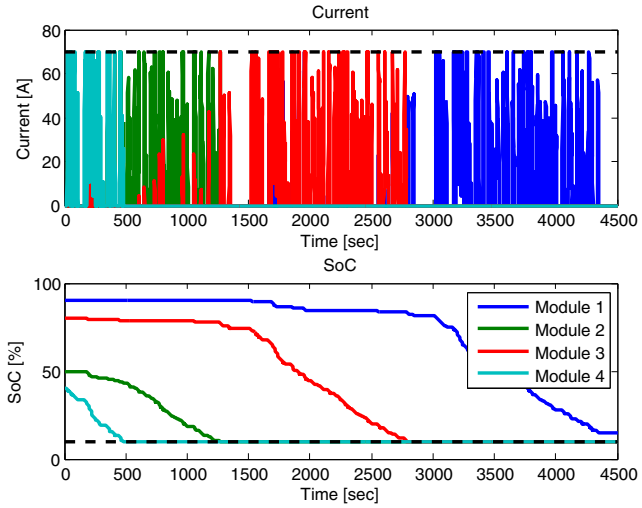

Fig. 8. SeqD Scheduling for Dynamic Power Demand

and sequential discharge scheduling algorithms are introduced, then the hybrid discharge scheduling algorithm is executed by solving a QP problem. These algorithms are demonstrated by constant current demand simulations. The hybrid scheduling not only decreases the energy loss due to internal resistance but also results in sequential depletion of battery modules that enhances the flexibility of the battery system.

Applications of current scheduling for parallel connected battery systems with different operating parameters can be found in BEVs with exchangeable battery modules or second life battery systems for ancillary grid services. The paper shows how a UDDS driving profile is scheduled with 4 parallel modules. Optimization algorithms such as Semidefinite Programming (SDP) can be utilized for scheduling for dynamic power demand, which aims to minimize the total energy consumption of the battery system.

REFERENCES

Armand, M. and Taracson, J.M. (2008). Building better batteries. *Nature*, 451, 652–657.

Bai, X., Wei, H., Fujisawa, K., and Wang, Y. (2008). Semidefinite programming for optimal power flow problems. *Electrical Power and Energy Systems*, 30, 383–392.

Botsford, C. and Szczepanek, A. (2009). Fast charging vs. slow charging: Pros and cons for the new age of electric vehicles. In *Proceeding of Electric Vehicle Symposium 24*. Stavanger, Norway.

Bragard, M., Soltau, N., Thomas, S., and Doncker, R.W.D. (2010). The balance of renewable sources and user demands in grids - power electronics for modular battery energy storage systems. *IEEE Transactions on Power Electronics*, 25, 3049–3056.

Chaturvedi, N.A., Klein, R., Christensen, J., Ahmed, J., and Kojic, A. (2010). Algorithms for advanced battery-management systems. *IEEE Control Systems*, 30, 49–68.

Coleman, T.F. and Li, Y. (1996). A reflective newton method for minimizing a quadratic function subject to bounds on some of the variables. *SIAM Journal on Optimization*, 6, 1040–1058.

Gao, L., Liu, S., and Dougal, R.A. (2002). Dynamic lithium-ion battery model for system simulation. *IEEE Transactions on Components and Packing Technologies*, 25(3), 495–505.

Kaiser, R. (2007). Optimized battery-management system to improve storage lifetime in renewable energy systems. *Journal of Power Sources*, 168, 58–65.

Kang, B. and Ceder, G. (2009). Battery materials for ultrafast charging and discharging. *Nature*, 452, 190–193.

Khaligh, A. and Li, Z. (2010). Battery, ultracapacitor, fuel cell, and hybrid energy storage systems for electric, hybrid electric, fuel cell, and plug-in hybrid electric vehicles: State of the art. *IEEE Transactions on Vehicular Technology*, 59(6), 2806–2814.

Lacey, G., Putrus, G., and Salim, A. (2013). The use of second life electric vehicle batteries for grid support. In *Proceeding of IEEE EuroCon*. Zagreb, Croatia.

Lin, X., Stefanopoulou, A.G., Li, Y., and Anderson, R.D. (2013). State of charge estimation of cells in series connection by using only the total voltage measurement. In *Proceedings of the 2013 American Control Conference*, 1908–1913. Washington DC, USA.

Mehrotra, S. (1992). On the implementation of a primal-dual interior point method. *SIAM Journal of Optimization*, 2, 575–601.

Moura, S.J., Chaturvedi, N.A., and Krstic, M. (2012). PDE estimation techniques for advanced battery management systems - Part I: SOC estimation. In *Proceedings of the 2012 American Control Conference*, 559–565. Montreal, Canada.

Nishi, Y. (2001). Lithium ion secondary batteries: past 10 years and the future. *Journal of Power Resource*, 100, 101–106.

Sitterly, M., Wang, L.Y., Yin, G.G., and Wang, C. (2011). Enhanced identification of battery models for real-time battery management. *IEEE Transactions on Sustainable Energy*, 2, 300–308.

Smith, K. and Wang, C.Y. (2006). Power and thermal characterization of a lithium-ion battery pack for hybrid-electric vehicles. *Journal of Power Sources*, 160, 662–673.

Ye, Y. (2002). *Handbook of Applied Optimization: Quadratic Programming*. Oxford University Press.